Survey of heavy-ion fusion hindrance for lighter systems

C. L. Jiang, K. E. Rehm, B. B. Back, and R. V. F. Janssens

Physics Division, Argonne National Laboratory, Argonne, Illinois 60439, USA

(Received 2 February 2009; published 7 April 2009)

A survey of heavy-ion fusion cross sections at extreme sub-barrier energies has been carried out for lighter systems with positive Q values. A general parametrization is proposed, which describes excitation functions for a wide range of light systems at low energies. This parametrization is then applied to a calculation of excitation functions and S factors for the system $^{16}O + ^{16}O$, which has recently been investigated with various other theoretical approaches. It is suggested that this parametrization is useful for estimating sub-barrier fusion cross sections with exotic neutron-rich partners which cannot be studied in the laboratory.

I. INTRODUCTION

Fusion reactions between lighter heavy ions are very important in explosive stellar burning processes. Reactions such as $^{12}C + ^{12}C$, $^{12}C + ^{16}O$, and $^{16}O + ^{16}O$ are the main processes during the carbon and oxygen burning stages. Furthermore, other fusion reactions, e.g., $^{24}O + ^{24}O$, $^{28}Ne + ^{28}Ne$, and $^{34}Ne + ^{34}Ne$ are involved in the evolution of the inner crust of accreting neutron stars [1,2], and an evaluation of the relevant cross sections is desirable. It was pointed out [3] that heavy-ion fusion hindrance will be very important if this phenomenon also occurs in fusion reactions between lighter heavy ions. Since a full understanding of fusion hindrance has not yet been achieved, it is worthwhile to develop a phenomenological systematics of the hindrance behavior for these lighter heavy-ion reactions.

Heavy-ion fusion hindrance was first observed in medium-mass systems at extreme sub-barrier energies [4–7]. A steep fall off of the fusion cross section was observed at very low energies and, correspondingly, an S factor maximum appeared [8]. Subsequent measurements and analyses have shown that this hindrance may be a general feature of heavy-ion fusion reactions at extreme sub-barrier energies [9–11].

Excitation functions for fusion reactions induced by ^{12}C and ^{16}O ions at energies of astrophysical interest have recently been reevaluated by including heavy-ion fusion hindrance contributions [12]. The impact on the results for carbon and oxygen burning and the influence on nucleosynthesis have been discussed in Ref. [13]. While none of these reactions has been measured down to energies where a maximum of the S factor should appear, recent experiments for a heavier fusion system with a positive Q value, $^{28}Si + ^{30}Si$ ($Q = 14.3$ MeV), [14] support the conclusion that the hindrance phenomenon does occur also in fusion systems with positive Q values. However, in order to fully understand the fusion hindrance behavior and to obtain better extrapolations, the reactions $^{12}C + ^{12}C$, $^{12}C + ^{16}O$, and $^{16}O + ^{16}O$ have to be measured to lower energies than is the case so far [15]. Extrapolations are especially important for reactions with unstable nuclei, e.g., $^{24}O + ^{24}O$, $^{28}Ne + ^{28}Ne$, $^{34}Ne + ^{34}Ne$, $^{32}Mg + ^{32}Mg$, etc., which will be impossible to measure in the laboratory in the foreseeable future. Their excitation functions and reaction

rates will have to come from theoretical calculations (as done in Refs. [16–18]).

In our previous papers [8,11,19], we have shown that the onset of sub-barrier fusion hindrance can be identified by the appearance of a maximum in the S factor at an energy E_s or by an intersection between the logarithmic derivative, $L(E) = d \ln(\sigma E)/dE$ and the constant S factor function, $\pi \eta / E$ at L_s and E_s, both of which depend systematically on an entrance channel parameter $\zeta = Z_1 Z_2 \sqrt{\mu}$, where $\mu = A_1 A_2 / (A_1 + A_2)$. The systematics of the parameters E_s and L_s has been already developed in Refs. [8,11,19]. In this work, we will develop the systematics of the parameters A_0 and B_0, which describe the shapes of the S factor and the logarithmic derivative $L(E)$ near E_s (see below). These parameters are important for the extrapolation of the excitation functions to lower energies, and they can also be expressed as functions of the entrance channel variable $\zeta = Z_1 Z_2 \sqrt{\mu}$.

The variable ζ describes the system dependence of the Sommerfeld parameter η when it is expressed as a function of the center-of-mass energy, E:

$$\eta = \frac{Z_1 Z_2 e^2}{\hbar v} = \frac{e^2 \zeta}{\hbar \sqrt{2E}}. \qquad (1)$$

The Sommerfeld parameter η plays an important role in the barrier penetration (Gamow factor),

$$\exp(-2\pi\eta) = \exp\left(-\frac{\sqrt{2}\pi e^2}{\hbar} \frac{\zeta}{\sqrt{E}}\right), \qquad (2)$$

as well as in the Coulomb wave functions $F_l(r)$ and $G_l(r)$, whose asymptotic values (at $r \to \infty$) can be expressed as

$$F_l(r) \to \sin\left(kr - \frac{l\pi}{2} - \eta \ln 2kr + \sigma_l\right), \qquad (3)$$

and

$$G_l(r) \to \cos\left(kr - \frac{l\pi}{2} - \eta \ln 2kr + \sigma_l\right), \qquad (4)$$

where the Coulomb phase shift σ_l depends also on the parameter η.

II. SYSTEMATICS OF HEAVY-ION FUSION HINDRANCE FOR SYSTEMS WITH A POSITIVE Q VALUE

For the description of heavy-ion fusion cross sections at very low energies, two representations have been developed [4,8]. Converting the cross sections into an S factor ($S(E) = \sigma E \exp(2\pi\eta)$) eliminates the strong energy dependence originating from tunneling through the Coulomb barrier. The choice of the logarithmic derivative, $L(E)$, on the other hand is useful especially for a comparison of fusion cross sections obtained by different groups, since it eliminates normalization and efficiency errors in the experimental data. In the following we will, therefore, use both parametrizations, although the parameters obtained in the two representations are clearly not independent.

For the logarithmic derivative $L(E)$ an extrapolation function was suggested in Ref. [12] given by

$$L(E) = A_0 + \frac{B_0}{E^{N_p}} \text{ (MeV}^{-1}), \tag{5}$$

where N_p is assumed to be 1.5, and A_0 and B_0 are the two fit parameters. The choice of the exponent is somewhat arbitrary. Since the energy dependence of a constant S factor is $\sim E^{-3/2}$, the factor $N_p = 1.5$ was chosen for our parametrization. In practice, we found that Eq. (5) describes the experimental data well. The same exponent was also chosen by Fowler *et al.* [20] in their representation of fusion cross sections at low energies. The parameters E_s and L_s can then be determined directly from A_0 and B_0 with the equations

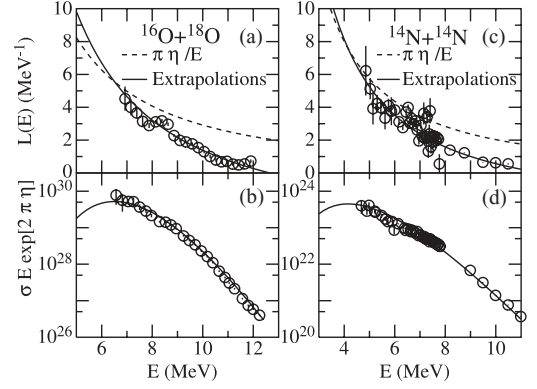$$E_s = \left(\frac{0.495\zeta - B_0}{A_0}\right)^{2/3} \text{ (MeV)}, \tag{6}$$

FIG. 1. (a),(c) Plots of the logarithmic derivative $L(E)$ versus center-of-mass energy E for the reactions $^{16}\text{O} + ^{18}\text{O}$ and $^{14}\text{N} + ^{14}\text{N}$, respectively. (b),(d) Plots for $S(E)$ versus E for these two reactions. Solid curves are fits of $L(E)$ with the equation $L(E) = A_0 + B_0/E^{1.5}$ for the low energy parts of the data [in (a),(c)], and the corresponding extrapolations of $S(E)$ [in (b),(d)]. Dashed curves are obtained by assuming a constant S factor.

and

$$L_s = \frac{0.495\zeta A_0}{0.495\zeta - B_0} \text{ (MeV}^{-1}). \tag{7}$$

The corresponding extrapolated cross section $\sigma(E)$ can then be expressed as [12]

$$\sigma(E) = \sigma_s \frac{E_s}{E} e^{[A_0(E-E_s) - B_0 \frac{1}{E_s^{N_p-1}} \frac{1}{(N_p-1)}((\frac{E_s}{E})^{N_p-1}-1)]}. \tag{8}$$

This equation will be used later in the S factor representation. Here the parameter σ_s is the cross section at the S factor

TABLE I. Results obtained from least-squares fits to the low-energy data of the logarithmic derivative $L(E)$ and S factor for reactions with positive Q values for fusion. Some of the data have already been discussed in Refs. [11,12,14,19]. E_s and L_s are the values of the energy and the logarithmic derivative at the point where $S(E)$ exhibits a maximum. A_0 and B_0 are obtained from least-squares fits with the equation $L(E) = A_0 + B_0/E^{1.5}$. σ_s is the value of the fitted cross section at the maximum of the S factor (for details see Ref. [12]). The parameters E_s and L_s and their uncertainties have been obtained from Eqs. (6) and (7). For this reason, some of the values and uncertainties are small different from the ones presented previously. The fusion Q values and entrance channel variable, $\zeta = Z_1 Z_2 \sqrt{\mu}$ are included for reference.

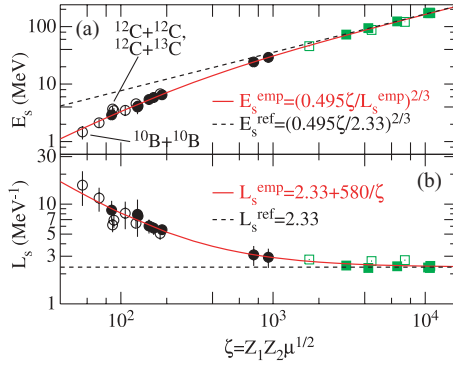| System	E_s MeV	L_s MeV^{-1}	A_0 MeV^{-1}	B_0 MeV$^{1/2}$	σ_s mb	Q MeV	ζ	Ref.
$^{16}\text{O} + ^{76}\text{Ge}$	29.1(4.2)	2.93(0.64)	−6.86(1.2)	1538.(138.)	0.0052	10.504	930.7	[37]
$^{28}\text{Si} + ^{30}\text{Si}$	24.2(3.6)	3.10(0.70)	−6.48(0.95)	1141.(132.)	0.012	14.302	745.6	[14]
$^{16}\text{O} + ^{18}\text{O}$	6.51(0.35)	5.54(0.50)	−3.24(0.13)	146.1(3.8)	0.0030	24.413	186.3	[21]
$^{16}\text{O} + ^{16}\text{O}$	6.78(0.62)	5.07(0.69)	−4.11(0.71)	162.1(15.4)	0.0080	16.542	181.0	[21,22,27,28]
$^{12}\text{C} + ^{20}\text{Ne}$	5.85(0.56)	5.74(0.83)	−2.20(0.21)	112.4(6.7)	4.6×10^{-4}	18.974	164.3	[22]
$^{14}\text{N} + ^{16}\text{O}$	5.39(0.58)	6.04(0.97)	−2.25(0.27)	103.9(6.8)	5.2×10^{-4}	18.327	153.0	[23]
$^{14}\text{N} + ^{14}\text{N}$	4.15(0.31)	7.59(0.82)	−2.00(0.06)	81.03(1.62)	4.8×10^{-5}	27.220	129.6	[24]
$^{13}\text{C} + ^{16}\text{O}$	4.00(0.16)	7.9(3.2)	−2.06(0.35)	80.17(6.10)	6.4×10^{-5}	20.283	128.6	[25]
$^{12}\text{C} + ^{16}\text{O}$	4.54(0.27)	6.43(0.57)	−2.08(0.12)	82.35(2.90)	0.0012	16.756	125.7	[29–31]
$^{12}\text{C} + ^{14}\text{N}$	3.49(0.71)	8.1(2.5)	−1.80(0.43)	64.56(6.79)	1.5×10^{-4}	15.074	106.8	[32]
$^{12}\text{C} + ^{13}\text{C}$	3.45(0.37)	6.9(1.1)	−2.32(0.24)	59.37(2.25)	0.015	16.318	89.9	[33]
$^{12}\text{C} + ^{12}\text{C}$	3.68(0.38)	6.18(0.95)	−1.32(0.12)	52.93(1.15)	0.023	13.934	88.2	[34–36]
$^{11}\text{B} + ^{14}\text{N}$	2.90(0.47)	8.7(2.1)	−1.75(0.18)	51.64(1.90)	0.00057	24.724	86.9	[26]
$^{11}\text{B} + ^{12}\text{C}$	2.12(0.38)	11.5(3.1)	−1.81(0.21)	41.17(1.37)	9.3×10^{-5}	18.198	71.9	[32]
$^{10}\text{B} + ^{10}\text{B}$	1.47(0.38)	15.5(5.9)	−2.17(0.70)	31.55(10.8)	2.2×10^{-5}	31.143	55.9	[32]

FIG. 2. (Color online) (a) Plot of E_s versus ζ for several heavy-ion fusion systems. The Q values for fusion are positive or negative for those systems which are described by black circles or green squares, respectively. The eight solid circles are for systems analysed in the present work. (b) Similar plot for L_s versus ζ.

maximum. This approach for E_s, L_s, A_0, B_0, and σ_s has already been used previously in the analysis of some systems with positive Q values for fusion [11,12,14,19].

We now apply this extrapolation to other systems with positive Q values: $^{16}O + {}^{18}O$ [21], $^{12}C + {}^{20}Ne$ [22], $^{14}N + {}^{16}O$ [23], $^{14}N + {}^{14}N$ [24], $^{13}C + {}^{16}O$ [25], and $^{11}B + {}^{14}N$ [26]. Plots of the logarithmic derivatives $L(E)$ and of the $S(E)$ factors versus the energy E are presented in Fig. 1 for the systems $^{16}O + {}^{18}O$ and $^{14}N + {}^{14}N$. Here, the experimental logarithmic derivatives are obtained from least-squares fits to three or four consecutive data points of cross sections, respectively. The fits and extrapolations using Eqs. (5) and (8) (solid curves) reproduce the experimental data quite well. The parameters obtained for all the systems with positive Q values are listed in Table I. The parameters for the systems $^{16}O + {}^{16}O$, $^{12}C + {}^{16}O$, $^{12}C + {}^{14}N$, $^{12}C + {}^{13}C$, $^{12}C + {}^{12}C$, $^{11}B + {}^{12}C$, and $^{10}B + {}^{10}B$ have been taken from Ref. [19]. The system $^{16}O + {}^{76}Ge$ [37], with a fusion Q value of 10.504 MeV, is also included in the present paper. It was treated previously in [19] using a linear extrapolation. Thus, there are small differences in the values of E_s and L_s between the present and the previous paper [19]. The results for the reaction $^{28}Si + {}^{30}Si$ were taken from Ref. [14].

Plots of E_s and L_s versus the entrance channel parameter $\zeta = Z_1 Z_2 \sqrt{\mu}$ are presented in Fig. 2. Empirical functions

$$L_s^{\mathrm{emp}} = 2.33 + 580/\zeta \ (\mathrm{MeV}^{-1}), \tag{9}$$

and

$$E_s^{\mathrm{emp}} = \left(0.495\zeta/L_s^{\mathrm{emp}}(\zeta)\right)^{2/3} \ (\mathrm{MeV}), \tag{10}$$

developed in Refs. [8,11,19], are shown by the solid lines in Fig. 2.[1] The new results (solid circles) are described well by these curves. The dashed lines in Fig. 2 represent the previous empirical functions (L_s^{ref} and E_s^{ref}), which were developed for a description of heavier mass systems and do not include the
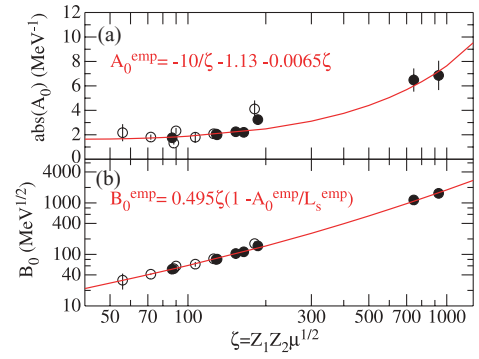
FIG. 3. (Color online) (a) Plot of A_0 versus ζ for lighter heavy-ion reactions. (b) Similar plot for B_0 versus ζ. Here, only systems with positive Q values are included. The eight solid circles are obtained from the present work.

factor $580/\zeta$ in Eq. (9). This term has a negligible influence for systems with large values of ζ, corresponding to systems with large negative Q values for fusion. They are included in Fig. 2 for comparison. It should be noted that Eqs. (9) and (10) are valid for systems with either positive or negative Q values for fusion.

Plots of the parameters A_0 and B_0 as a function of ζ are given in Fig. 3. They exhibit rather regular trends as a function of the entrance channel parameter ζ. The solid line in Fig. 3(a) is obtained from the empirical equation

$$A_0^{\mathrm{emp}} = -10/\zeta - 1.13 - 0.0065\zeta \ (\mathrm{MeV}^{-1}). \tag{11}$$

In principle, the two parameters A_0 and B_0 are related by Eq. (5). As a result, the empirical function B_0^{emp} can be expressed by using Eqs. (9), (10), and (11):

$$B_0^{\mathrm{emp}}(\zeta) = 0.495\zeta \left(1 - A_0^{\mathrm{emp}}(\zeta)/L_s^{\mathrm{emp}}(\zeta)\right) \ (\mathrm{MeV}^{1/2}), \tag{12}$$

as shown by the solid curve in Fig. 3(b). Equations (11) and (12) reproduce the data for A_0 and B_0 as a function of ζ rather well. Equations (11) and (12) as well as Eqs. (5) and (8) can only be used for systems with positive Q values. For negative Q values, a modification to Eq. (5) is needed.[2]

Equations (9), (10), (11), and (12) form a set of functions $E_s^{\mathrm{emp}}(\zeta)$, $L_s^{\mathrm{emp}}(\zeta)$, $A_0^{\mathrm{emp}}(\zeta)$, and $B_0^{\mathrm{emp}}(\zeta)$, which can be used to predict the shape of the excitation function at very low energies, including the contributions from fusion hindrance. It should be noted that among these four equations, only Eqs. (9) and (11) are independent.

Another parameter, σ_s, is needed to obtain the absolute cross section of the extrapolated part of the excitation function. The values of σ_s are summarized in Table I and are plotted in Fig. 4 as a function of the entrance channel variable ζ. Contrary to the parameters E_s, L_s, A_0, and B_0 which show smooth dependences on the parameter ζ, σ_s exhibits variations by as much as three orders of magnitude. The highest values for σ_s are observed for the systems $^{12}C + {}^{12}C$, $^{12}C + {}^{13}C$, and $^{16}O + {}^{16}O$, whereas σ_s is very low for $^{10}B + {}^{10}B$ and $^{14}N + {}^{14}N$. These variations can be understood from Eq. (8),

---

[1]Because more data are included, the value of the second parameter in Eq. (9) is 580 instead of 500. The later, 500, was used in the Eq. (6) of Ref. [19].

[2]For systems with a negative Q value, equation $A_0 + \frac{B_0}{(E+Q)^{1.5}}$ should be used instead of Eq. (5), see also, for example, Ref. [12] for details.
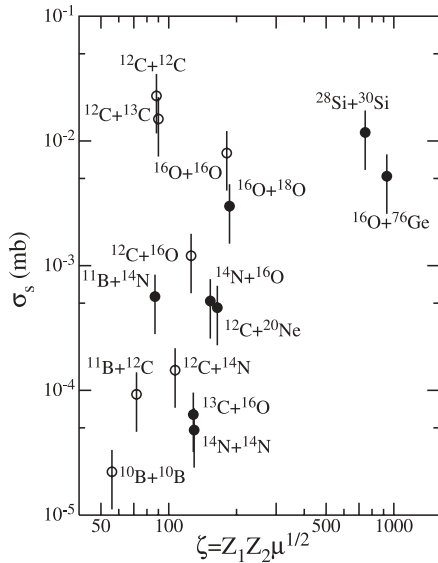
FIG. 4. Plot of σ_s versus ζ for heavy-ion fusion reactions with positive Q values. Because the uncertainties associated with fusion cross sections at low energies are quite significant (see for example Fig. 5) a universal uncertainty of 50% has been assigned to all σ_s values in this figure.

which indicates that $\sigma(E)$ depends linearly on σ_s but exponentially on the parameters E_s, A_0, and B_0. Nuclear structure effects can easily lead to small deviations of, e.g., E_s from the empirical curve $E_s^{\mathrm{emp}}(\zeta)$ (as indicated in Fig. 2), which, when magnified through the exponential behavior, lead to a strong correlation between σ_s and $E_s - E_s^{\mathrm{emp}}$. A large positive difference $E_s - E_s^{\mathrm{emp}}$ corresponds to a large σ_s and a large negative $E_s - E_s^{\mathrm{emp}}$ value is associated with a small value of σ_s. Though the correlation between σ_s and $E_s - E_s^{\mathrm{emp}}$ can be found in the data listed in Table I, the influence of nuclear structure on the hindrance behavior, e.g., the α cluster structure and the odd-even mass effects are not
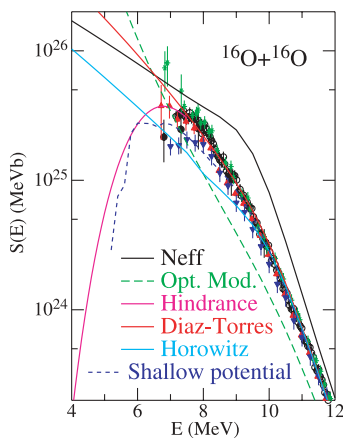

FIG. 5. (Color) Comparison between experimental data and various recent model calculations in a plot of $S(E)$ versus E for the $^{16}\mathrm{O} + {}^{16}\mathrm{O}$ system. The experimental data are taken from the literature: black open and solid circles: Spinka *et al.* [27]; green stars: Hulke *et al.* [22]; red upward triangles: Thomas *et al.* [21]; blue downward-triangles: Wu *et al.* [28].

well understood. Furthermore, contributions from resonances, which are important for reactions involving nuclei such as $^{12}\mathrm{C}$ and $^{16}\mathrm{O}$, are not included in this global analysis. Therefore, only the shape of the low energy part of the excitation function can be predicted by the parametrization described above.

III. COMPARISON WITH RECENT CALCULATIONS FOR THE REACTION $^{16}\mathrm{O} + {}^{16}\mathrm{O}$

A detailed comparison of previous extrapolations with experimental data for the reaction $^{16}\mathrm{O} + {}^{16}\mathrm{O}$ has been presented in Ref. [12]. Since then, several new calculations have been performed; these are summarized in Fig. 5. The earlier extrapolations, e.g., by Fowler *et al.* [20], Hulke *et al.* [22], Gasques *et al.* [38], etc., are not included.

The experimental data taken from various sources [21,22, 27,28] agree for center of mass energies above $E \sim 9$ MeV, but exhibit large differences, by up to a factor of 4, for $E \sim 7$ MeV. The results of optical model calculations using a standard average potential ($V = 50$ MeV, $W = 10$ MeV, $r_0 = r_{0i} = 1.28$ fm and $a_0 = a_i = 0.4$ fm, [32,39]) are shown by the green dashed curve. These calculations predict an exponentially growing S factor. At the higher energies, their slope is in agreement with the slope of the data, but the absolute values of the S factor are underpredicted by factors of 2–3. These calculations predict the highest S factors at the astrophysical important energies, $E \leqslant 3.67$ MeV ($T_9 \leqslant 1$). Recently, Neff *et al.* [17] have calculated fusion cross sections for the systems $^{16}\mathrm{O} + {}^{16}\mathrm{O}$, $^{22}\mathrm{O} + {}^{22}\mathrm{O}$, and $^{24}\mathrm{O} + {}^{24}\mathrm{O}$ within the fermionic molecular dynamics model. Their calculations for $^{16}\mathrm{O} + {}^{16}\mathrm{O}$ are represented by the black curve in Fig. 5. Although the wave functions used in these calculations are fully antisymmetrized products of frozen ground states and, therefore, saturation effects should be included explicitly, no maximum, but only a change in the slope of the S factor at $E \sim 9.5$ MeV is observed. In addition, the absolute values of the S factor are overpredicted by factors of 2–3 over most of the energy range. A similar change in the slope of the S factor is predicted at $E \sim 9.5$ MeV by Horowitz *et al.* [18], who calculated the astrophysical S factors for the reactions $^{24}\mathrm{O} + {}^{24}\mathrm{O}$ and $^{28}\mathrm{Ne} + {}^{28}\mathrm{Ne}$, as well as for $^{16}\mathrm{O} + {}^{16}\mathrm{O}$, $^{12}\mathrm{C} + {}^{16}\mathrm{O}$, and $^{12}\mathrm{C} + {}^{12}\mathrm{C}$ using a barrier penetration model. Their result is given by the light blue curve. Their calculations are in good agreement with the data at higher energies, down to about 10 MeV. At lower energies, the S factor is underpredicted by about a factor of 2 to 3. The best overall agreement between data and theory is observed by Diaz-Torres *et al.* [40], who have calculated the $S(E)$ factor for $^{16}\mathrm{O} + {}^{16}\mathrm{O}$ using a realistic two-center shell model, as shown by the brown curve. While these three new calculations do not predict an S factor maximum, they all predict a change in slope when compared to optical model predictions.

The S factor prediction for the system $^{16}\mathrm{O} + {}^{16}\mathrm{O}$, with the inclusion of the hindrance behavior [12], is indicated by the magenta curve. It has an S factor maximum and reproduces the trend of the experimental data at low energies satisfactorily.

For medium-mass systems, the hindrance phenomenon was explained by Mişicu and Esbensen [41] through the inclusion

of the saturation property of nuclear matter. This results in a model with a shallow potential, which can also reproduce the experimental results for a system with positive Q value, ^{28}Si + ^{30}Si [14]. This shallow potential model has recently been used to calculate fusion in light heavy-ion reactions [42]. The results for the system ^{16}O + ^{16}O are given by the blue dashed curve in Fig. 5 and a maximum in the S factor is also predicted.

There are a few more recent calculations for the fusion reaction ^{16}O + ^{16}O, (see, e.g., Ref. [16]). Because these results are very similar to the three calculations mentioned above, they have not been included in the discussion.

From Fig. 5 it is clear that the main differences between the various predictions occur for energies below $E \sim 7$ MeV, in the experimentally unmeasured region. For this reason an extension of excitation function measurements toward lower energies is urgently needed [15].

IV. CONCLUDING REMARKS

The low-energy behavior of heavy-ion fusion cross sections of interest in nuclear astrophysics has been surveyed. Since no fusion experiments at astrophysical energies have yet been performed for these systems, one has to rely on extrapolation techniques. In the past, all these extrapolations used optical model calculations which predicted a continuously rising S factor. On the other hand, recent fusion experiments with medium-mass systems have revealed a hindrance of the fusion cross section which leads to a maximum of the S factor,

followed by a decrease toward lower energies. For these medium-mass systems, which all have negative Q values, a maximum of the S factor should be expected because of energy conservation. While this hindrance has been associated with the incompressibility of nuclear matter at large density overlaps [41], a fully reliable theoretical description of the cross sections at sub-barrier energies has yet to be developed. Extending the systematics developed at first for systems with a negative Q value to the fusion of light heavy ions leads to cross sections which are quite different from the ones obtained from optical model calculations. Other calculations within the frameworks of the two-center shell model or fermionic molecular dynamics give cross sections which are intermediate between the optical model and the fusion hindrance predictions. Further experiments at lower energies are clearly needed to test these theories. These are difficult and time-consuming measurements and, for this reason, a parametrization of the sub-barrier fusion cross sections such as the one developed in this paper will be useful for the prediction of fusion cross sections of exotic reactions, which remain outside present experimental capabilities. The validity of such a prediction has, of course, to be tested in future experiments.

[1] P. Haensel and J. L. Zdunik, Astron. Astrophys. **229**, 117 (1990); **404**, L33 (2003).

[2] C. J. Horowitz, D. K. Berry, and E. F. Brown. Phys. Rev. E **75**, 066101 (2007).

[3] M. Wiescher, AIP Conference Proceedings of Fusion08, Chicago, Sept. 22–26, 2008 (in press); D. Yakovlev, Bulletin of the American Physical Society, April Meeting of 2008, St. Louis, Missouri, (J14-1), p. 128.

[4] C. L. Jiang *et al.*, Phys. Rev. Lett. **89**, 052701 (2002).

[5] C. L. Jiang *et al.*, Phys. Rev. Lett. **93**, 012701 (2004).

[6] C. L. Jiang *et al.*, Phys. Rev. C **71**, 044613 (2005).

[7] C. L. Jiang *et al.*, Phys. Lett. **B640**, 18 (2006).

[8] C. L. Jiang, H. Esbensen, B. B. Back, R. V. F. Janssens, and K. E. Rehm, Phys. Rev. C **69**, 014604 (2004).

[9] M. Dasgupta, D. J. Hinde, A. Diaz-Torres, B. Bouriquet, C. I. Low G. J. Milburn, and J. O. Newton, Phys. Rev. Lett. **99**, 192701 (2007).

[10] M. Trotta *et al.*, Nucl. Phys. **A787**, 134c (2007).

[11] C. L. Jiang, B. B. Back, H. Esbensen, R. V. F. Janssens, and K. E. Rehm, Phys. Rev. C **73**, 014613 (2006).

[12] C. L. Jiang, K. E. Rehm, B. B. Back, and R. V. F. Janssens, Phys. Rev. C **75**, 015803 (2007).

[13] L. R. Gasques *et al.*, Phys. Rev. C **76**, 035802 (2007).

[14] C. L. Jiang *et al.*, Phys. Rev. C **78**, 017601 (2008).

[15] The Frontiers of Nuclear Science, A LONG RANGE PLAN, 2007, p. 72, http://www.er.doe.gov/np/nsac/does/Nuclear-Science.High-Res.pdf.

[16] L. R. Gasques, A. V. Afanasjev, M. Beard, J. Lubian, T. Neff, M. Wiescher, and D. G. Yakovlev, Phys. Rev. C **76**, 045802 (2007).

[17] T. Neff, H. Feldmeier, and K. Langanke, arXiv:nucl-th/0703030v1.

[18] C. J. Horowitz, H. Dussan, and D. K. Berry, Phys. Rev. C **77**, 045807 (2008); H. Dussan *et al.* Bulletin of the American Physical Society, April Meeting 2008, St. Louis, Missouri, (D8-1), p. 53 (private communication).

[19] C. L. Jiang, B. B. Back, R. V. F. Janssens, and K. E. Rehm, Phys. Rev. C **75**, 057604 (2007).

[20] W. Fowler *et al.*, Annu. Rev. Astron. Astrophys. **13**, 69 (1975).

[21] J. Thomas, Y. T. Chen, S. Hinds, K. Langanke, D. Meredith, M. Olson, and C. A. Barnes, Phys. Rev. C **31**, 1980 (1985).

[22] G. Hulke *et al.*, Z. Phys. A **297**, 161 (1980).

[23] Z. E. Switkowski *et al.*, Nucl. Phys. **A279**, 502 (1977).

[24] Z. E. Switkowski *et al.*, Nucl. Phys. **A274**, 202 (1976).

[25] B. Dasmahapatra, B. Cujec, and F. Lahlou, Nucl. Phys. **A394**, 301 (1983).

[26] B. Dasmahapatra, B. Cujec, and F. Lahlou, Can. J. Phys. **61**, 657 (1983).

[27] H. Spinka *et al.*, Nucl. Phys. **A233**, 456 (1974).

[28] S. C. Wu *et al.*, Nucl. Phys. **A422**, 373 (1984); S. C. Wu, Ph.D. thesis, California Institute of Technology (1978).

[29] J. R. Patterson *et al.*, Nucl. Phys. **A165**, 545 (1971).

[30] B. Čujec and C. A. Barnes, Nucl. Phys. **A266**, 461 (1976).

[31] P. R. Christensen, Z. E. Switkowski, and R. A. Dayers, Nucl. Phys. **A280**, 189 (1977).

[32] R. G. Stokstad *et al.*, Phys. Rev. Lett. **37**, 888 (1976).

[33] R. A. Dayras *et al.*, Nucl. Phys. **A265**, 153 (1976).

[34] R. J. Patterson *et al.*, Astrophys. J. **157**, 367 (1969).

[35] M. Mazarakis *et al.*, Phys. Rev. C **7**, 1280 (1973).

[36] M. D. High and B. Čujec, Nucl. Phys. **A282**, 181 (1977).

[37] E. F. Aguilera, J. J. Kolata, and R. J. Tighe, Phys. Rev. C **52**, 3103 (1995).

[38] L. R. Gasques *et al.*, Phys. Rev. C **72**, 025806 (2005).

[39] G. J. Michaud and E. W. Vogt, Phys. Rev. C **5**, 350 (1972); G. J. Michaud, *ibid.* **8**, 525 (1973).

[40] A. Diaz-Torres, L. R. Gasques, and M. Wiescher, Phys. Lett. **B652**, 255 (2007).

[41] S. Mişicu and H. Esbensen, Phys. Rev. Lett. **96**, 112701 (2006).

[42] H. Esbensen, Phys. Rev. C **77**, 054608 (2008).